Journal of Photochemistry and Photobiology A: Chemistry 221 (2011) 154–159

Contents lists available at ScienceDirect

Journal of Photochemistry and Photobiology A: Chemistry

journal homepage: www.elsevier.com/locate/jphotochem

Spatial distribution of enhanced optical fields in monolayered assemblies of metal nanoparticles: Effects of interparticle coupling

Hiromi Okamoto[a,*], Kohei Imura[b,c], Toru Shimada[d], Masahiro Kitajima[e]

[a] Department of Photo-Molecular Science, Institute for Molecular Science and The Graduate University for Advanced Studies, 38 Nishigonaka, Myodaiji, Okazaki, Aichi 444-8585, Japan
[b] Department of Chemistry and Biochemistry, School of Science and Engineering, Waseda University, Okubo, Shinjuku, Tokyo 169-8555, Japan
[c] PRESTO, Japan Science and Technology Agency, Honcho, Kawaguchi, Saitama 332-0012, Japan
[d] Fritz-Haber-Institut der Max-Planck-Gesellschaft, Faradayweg 4-6, D-14195 Berlin, Germany
[e] Department of Applied Physics, School of Applied Sciences, National Defense Academy of Japan, 1-10-20 Hashirimizu, Yokosuka, Kanagawa 239-8686, Japan

ARTICLE INFO

Article history:
Available online 1 February 2011

Keywords:
Near-field optical microscopy
Surface plasmon resonance
Metal nanoparticles
Enhanced optical fields
Surface enhanced Raman scattering
Finite-difference time-domain (FDTD) method

ABSTRACT

Near-field two-photon excitation images of assemblies of many gold nanospheres show characteristic feature that enhanced optical fields are confined at the rim parts of the assemblies. In the present report we analyzed the origin of this feature based on finite-difference time-domain (FDTD) approach as well as a simple point dipole model that incorporates the interparticle interaction with the dipole–dipole potential. It has been found that the simple point dipole model is useful for qualitative discussion on the optical field distribution in the metal nanoparticle assemblies. From the analysis, we have found that the interparticle interaction, which causes the propagation of the plasmon excitation in the assemblies, seems to be essential for the localization of the enhanced field at the rim. We propose that regular close-packed assemblies do not yield efficiently enhanced optical fields in visible to near-infrared region, and rather assemblies with large fluctuation are more advantageous to get highly enhanced fields.

1. Introduction

It has been known that assembled noble metal nanoparticles give highly enhanced and confined electric fields at the interstitial sites between the particles, when the assembly is irradiated by light [1–8]. This characteristic is one of the major origins of surface-enhanced Raman scattering and various other surface-enhanced spectroscopies, which are extensively developed these decades [9]. Surface plasmon resonances have major contributions to the optical-field confinement mentioned above. The spatial scale of the confined electric field due to plasmon resonance is essentially smaller than the wavelength of light [10], and thus very high spatial resolution is necessary to directly observe the confined-field structure by optical methods. The conventional far-field optical microscopy is not useful for this purpose. Our research group showed that direct observation of localized optical fields in metal nanostructures is feasible by near-field imaging, especially by near-field two-photon excitation probability imaging method [11–16]. Dimers of spherical noble metal nanoparticles are regarded as prototypical systems for optical-field confinement and enhancement in the nanoparticle assemblies, and a number of theoretical works have been devoted to this topic [1,2,4–6,8]. It is theoretically predicted that an enhanced optical field (called 'hot spot') is confined at the interstitial site between the particles, when a dimer is irradiated by light polarized along the interparticle axis. It has been believed that strongly enhanced Raman scattering is observable when a Raman active molecule enters into such a hot spot. In our previous studies, we visualized the enhanced local optical fields in gold nanoparticle dimers to prove the existence of the hot spot, and at the same time showed that the localized fields indeed make major contribution to the enhanced Raman scattering [11,12]. Through these studies on prototypical metal-nanoparticle assemblies, the basic mechanism of surface-enhanced Raman scattering becomes clarified. Recently, far-field spectroscopic characteristics of assemblies composed of several particles with well-defined structures were also experimentally observed and were compared with the electromagnetic simulations [17,18]. Regular chain-structure assemblies of many metal nanoparticles were also studied theoretically [19,20].

On the other hand, the use of isolated dimers of nanoparticles (or other well-defined assemblies that consist of small number particles) is hardly considered in practical application of

* Corresponding author. Tel.: +81 564 55 7320; fax: +81 564 54 2254.
E-mail address: aho@ims.ac.jp (H. Okamoto).

1010-6030/$ – see front matter © 2011 Elsevier B.V. All rights reserved.
doi:10.1016/j.jphotochem.2011.01.017

surface-enhanced spectroscopies to high-sensitivity detections, and rather robust nanoparticle assemblies are preferable. A number of studies have been reported recently on fabrication of noble metal nanoparticle assemblies to get efficient enhancement of Raman scattering [21–26]. Efforts toward preparation of nearly close-packed assemblies have been sometimes reported to get higher Raman enhancements [21,22,25,26]. However, it is actually not clear whether the close-packed structures are really advantageous for Raman enhancements. To fabricate a metal nanostructure that reliably yields highly enhanced Raman scattering, it is essential to verify the spatial distribution of enhanced optical fields in the nanostructure. In our previous work, we studied optical field distribution for island-like monolayered many-particle assemblies of gold nanospheres, using the near-field two-photon excitation imaging technique [14]. We found that very strong enhancements were localized in the rim part of the island structures, although lower enhancements were found in the whole area of the assemblies.

Exploring the physical background for such field distributions may lead us to establish guidelines of designing nanostructures yielding highly efficient enhanced Raman scattering and photoreaction enhancements [27,28]. In this article, we report simulations of optical-field distributions for model structures of gold nanoparticle assemblies, based upon rigorous electromagnetic field calculations as well as upon a simple model considering inter-particle interactions. The simulated results are compared qualitatively with the near-field experimental results for the many-particle assemblies. On the basis of the simulation, the physical origin of the characteristic features of the optical field structures is discussed.

2. Method

In the present study, we try simulations of optical-field distributions in two ways described in the following, for the qualitative discussion of the characteristic features observed for the near-field two-photon excitation images of the monolayered island-like assemblies of gold nanospheres. In the first approach we calculate electric-field amplitudes for model structures of nanoparticle assemblies by the finite-difference time-domain (FDTD) method, a representative method of electromagnetic field simulation. We used commercial FDTD simulation software ("Poynting", Fujitsu Ltd.) for this purpose. Electric-field distribution upon far-field irradiation of light was calculated on the model structures (the details of the models are described below). A plane wave of electromagnetic field was irradiated from 500 nm above the monolayered assembly, and the electric-field amplitude on a plane 20 nm above the top surface of the particles was calculated. We adopted Berenger's perfectly matched layer (PML) condition [29] for the boundaries of the calculation area. For the dielectric function of gold, we used the reported value at 821 nm [30] and the Drude-type frequency dependence.

In another approach, we tried qualitative simulations of collective electromagnetic oscillation modes of the nanoparticle assemblies, based on a simple model where a particle was regarded as an oscillating point dipole. The assembly of the particles was ascribed as an ensemble of oscillating point dipoles that are coupled to each other through dipole–dipole interactions. On irradiation of light, surface plasmons are excited on the metal nanoparticles. In the model, a point dipole oscillating in the same frequency as the incident radiation field represents the plasmon excited on each metal nanoparticle. The direction of the dipole is assumed to coincide with the polarization direction of the incident light. All the dipoles on metal nanoparticles have identical eigen frequencies and amplitudes when the particles are isolated from the others. The plasmon excited on a particle interacts with plasmons on other particles through the dipole–dipole interaction potentials. As a result, the particle assembly forms collective plasmon modes, and each mode has different eigen frequency in general. The amplitude of each oscillating dipole a_i (i is the index of the particle) in the assembly satisfies the following eigen equation:

$$\mathbf{Ha} = E\mathbf{a} \tag{1}$$

$$\mathbf{a} = \begin{bmatrix} a_1 \\ a_2 \\ \vdots \\ a_N \end{bmatrix}$$

$$\mathbf{H} = \begin{bmatrix} \varepsilon & h_{12} & h_{13} & \cdots & h_{1N} \\ h_{21} & \varepsilon & h_{23} & \cdots & h_{2N} \\ & \cdots & \cdots & \cdots & \\ h_{N1} & h_{N2} & h_{N3} & \cdots & \varepsilon \end{bmatrix}$$

where ε denotes the eigen frequency of the dipole for the isolated particle (which can be set as 0 without loss of generality), and N is the number of the particles in the assembly. The off-diagonal term h_{ij} represents the interaction between particles i and j, and is assumed to be given by the following point dipole–point dipole interaction potential:

$$h_{ij} \sim \frac{\boldsymbol{\mu}_i \boldsymbol{\mu}_j}{|\mathbf{r}_{ij}|^3} - \frac{3(\boldsymbol{\mu}_i \mathbf{r}_{ij})(\boldsymbol{\mu}_j \mathbf{r}_{ij})}{|\mathbf{r}_{ij}|^5} = \frac{1 - 3\cos\theta_{ij}}{|\mathbf{r}_{ij}|^3} \tag{2}$$

where $\mathbf{r}_{ij}$ denotes a position difference vector between particles i and j, $\boldsymbol{\mu}_i$ represents the point dipole vector for particle i, and θ_{ij} is the angle between $\mathbf{r}_{ij}$ and the direction of the incident polarization. On the derivation of the final form of Eq. (2), we assumed that all the particles are associated with point dipoles of the same magnitudes and directions. We obtain the eigen frequency and the amplitudes of dipole oscillation on each particle, for individual collective oscillation mode, by solving the eigen equation Eq. (1). We define weighted local density of states on a particle i, ρ_i, at a frequency f as follows:

$$\rho_i = \sum_k \frac{{M_k}^2 {a_{ki}}^2}{(f - E_k)^2 + \gamma^2} \tag{3}$$

where a_{ki} and E_k represent the oscillating dipole amplitude of particle i and the eigen frequency, respectively, for kth eigen state, and γ is a parameter corresponding to the resonance-frequency width of the eigen modes. To facilitate comparison between the local density of states in this model and the field amplitude obtained by the FDTD simulation of the system under far-field irradiation, we included in Eq. (3) the weighting factor

$$M_k^2 = \left(\sum_i a_{ki} \right)^2 \tag{4}$$

which corresponds to the oscillator strength of mode k. With this treatment, the modes yielding no oscillating dipole as the whole assembly do not contribute to the weighted local density of states. The local density of states defined in this way gives spatial distribution of oscillating dipole that contribute to the far-field optical transition, and thus may correspond qualitatively to the electric-field distribution obtained by the FDTD simulation. The local density of states should be originally defined without the M_k^2 factor in Eq. (3), and the near-field images may correspond rather to this original definition of density of states. In the present study, however, we adopt the weighted density of states defined above, as we are also interested in comparison with the FDTD simulation results. The correspondence between the density of states as the

original definition and the near-field observation will be discussed in some other opportunity.

In this model (called hereafter "point dipole model") we assumed the simple dipole–dipole potential for the interparticle interaction, and it is obviously not satisfactory for quantitative discussion. This is a minimal model where interparticle interaction of vector character is incorporated. However, it may be still useful to clarify the physical origins of the characteristic spatial features of the field distribution observed. The advantages of this model over the advanced electromagnetic simulation like FDTD method lie in lower calculation cost as well as facility in getting an insight into physical picture of the phenomenon observed. The lower calculation cost enables analysis of assemblies composed of a large number of particles, which cannot be practically treated with FDTD method. The model also facilitates understanding the phenomenon with a clear physical picture, since it incorporates the interparticle interaction in a definite form of interaction potential (dipole–dipole potential in the present case), as we will give discussion in Section 3.2.

The simulations were conducted for the two-dimensionally assembled gold nanospheres whose structures are shown in Figs. 1A and 2A. One is a regular close-packed structure (Fig. 1A). The diameter of the particles and the gap distance between the particles were set to be 100 and 20 nm, respectively, for the FDTD simulation. In the point dipole model, oscillating point dipoles were placed at the centers of the spheres. In the other assembled structure, the above-mentioned close-packed structure was modified so as to introduce defects and fluctuation of the particle positions in the plane (Fig. 2A). The incident polarization for calculation was in *y*- (vertical) and *x*- (horizontal) directions for the regular structure and in *y*-direction for the disordered structure.

3. Results and discussion

3.1. Comparison of the results by the two simulation methods for the regular structure of assembly

Fig. 1 shows the results of simulations for the regular structure of gold nanosphere assembly obtained by the FDTD method (electric-field amplitude, Fig. 1B and D) and the point dipole model (local density of states, Fig. 1C and E). The field amplitude and the density of states are displayed in linear scales, and are normalized to their maxima in each panel. The spatial distribution of the field amplitude varies with oscillation frequency. Several representative images of field amplitudes obtained by the FDTD simulation are shown in the figure, along with the density-of-states images by the point dipole model, which qualitatively look similar to the FDTD images. The calculated electric fields (or densities of states) show symmetric spatial structures, reflecting the assumed regular and highly symmetric structure of the assembly. It may be worth noting, for the FDTD results at low frequencies (1667, 1154, and 1071 nm in Fig. 1B and D), that strong electric field is distributed in wide area of the inner part of the assembly. This tendency has a similarity to delocalization of electrons in low-energy molecular orbitals of a large molecule with a periodic structure. The similar tendency is also observable in the point dipole model. That is, the density of states is distributed widely in the inner part of the assembly for the low-frequency modes ($E = -3.58$ to -2.45 in Fig. 1C and E).

On the contrary, in the wavelength region around 1000–700 nm, strong field tends to be distributed in the outer parts (and outside) of the assembly in the FDTD results. In the point dipole model, the field distribution outside the assembly cannot be discussed. However, it seems that large amplitude of the dipole oscillation is not widely distributed in the inner part of the assembly in the frequency region around 0 ($E = -2.10$ to 1.82 in Fig. 1C and E). Although we cannot expect a quantitative accuracy in the point dipole model, it may be said that the density-of-states distribution reproduces qualitatively the features of the field structure obtained by the FDTD calculation. It is noteworthy that qualitatively similar spatial features appear in the same order for the FDTD method and the point dipole model on going from higher to lower frequency. In other words, the frequency order of the eigen modes by the FDTD calculation is roughly reproduced by the point dipole model. This finding indicates that the point dipole model incorporates to a certain degree the essential factors that determine optical field structures in the nanoparticle assemblies. Consequently, the point dipole model will help us to explore the physical origins of the spatial features of the optical fields obtained by near-field observations or by rigorous electromagnetic field calculations.

3.2. Field distribution for the disordered assembly and comparison with the near-field images

Fig. 2 shows simulated results of FDTD method and the point dipole model for the disordered assembly with defects and fluctuation of the structure. Again, the point dipole model yields the density-of-states distributions that qualitatively correspond to the electric fields simulated by FDTD method. As is similar to the regular structure, the electric field (or density of states) is relatively delocalized in the inner part of the assembly at the low frequency region. In the FDTD results (Fig. 2B/B′) in the wavelength region around 1000–700 nm, the strong optical fields are not found in the inner part, and are localized in the rim part of the assembly. The strong field is particularly confined in the dimer isolated from the rest of the assembly (upper right in Fig. 2A), and this tendency is well reproduced by the point dipole model (Fig. 2C/C′). At a higher frequency, the optical field is localized on the defect site in the FDTD simulation (625 nm), which is again reproduced by the point dipole model ($E = 1.50$). These results suggest that the point dipole model is useful for qualitative discussion of the optical field distribution observed by near-field measurements for the disordered large assemblies.

We have found a tendency on the density of states by the point dipole model, in the frequency region a little lower than 0, as described in the following. Fig. 3A shows some of representative examples. In these images, higher density of states is not distributed in the inner part of the assembly, and localized rather in the rim part. This tendency was maintained even when the assembly structure was partly modified. This tendency was actually found in the regular structures, but is particularly prominent for the disordered structures. In near-field two-photon excitation images of island-like assemblies of gold nanoparticles (Fig. 3B), enhanced optical fields are found to be confined in the rim part of the assemblies. This feature qualitatively coincides well with the tendency found for the point-dipole-model simulation. The wavelength of near-field two-photon excitation source was 785 nm, which is longer than the plasmon resonance wavelength for isolated gold nanospheres (around 530 nm). The result agrees again qualitatively well with the point dipole model. Since the point dipole model reproduces the observed tendency of the optical field distribution, we may consider that the model correctly incorporates, at least qualitatively, the physical origin of the field confinement at the rim part of the assembly. The essential factor of the point dipole model is that the plasmon excited on a particle interacts with other particles through the dipole–dipole potential. Due to this interaction, the plasmon on a particle can transfer to other near-by particles (i.e., the excitation propagates). In the inner parts of the two-dimensional many-particle assemblies, the plasmon excitations on the particles propagate to peripheries and thus do not localize at certain sites, and this behavior may be the reason why strong optical fields

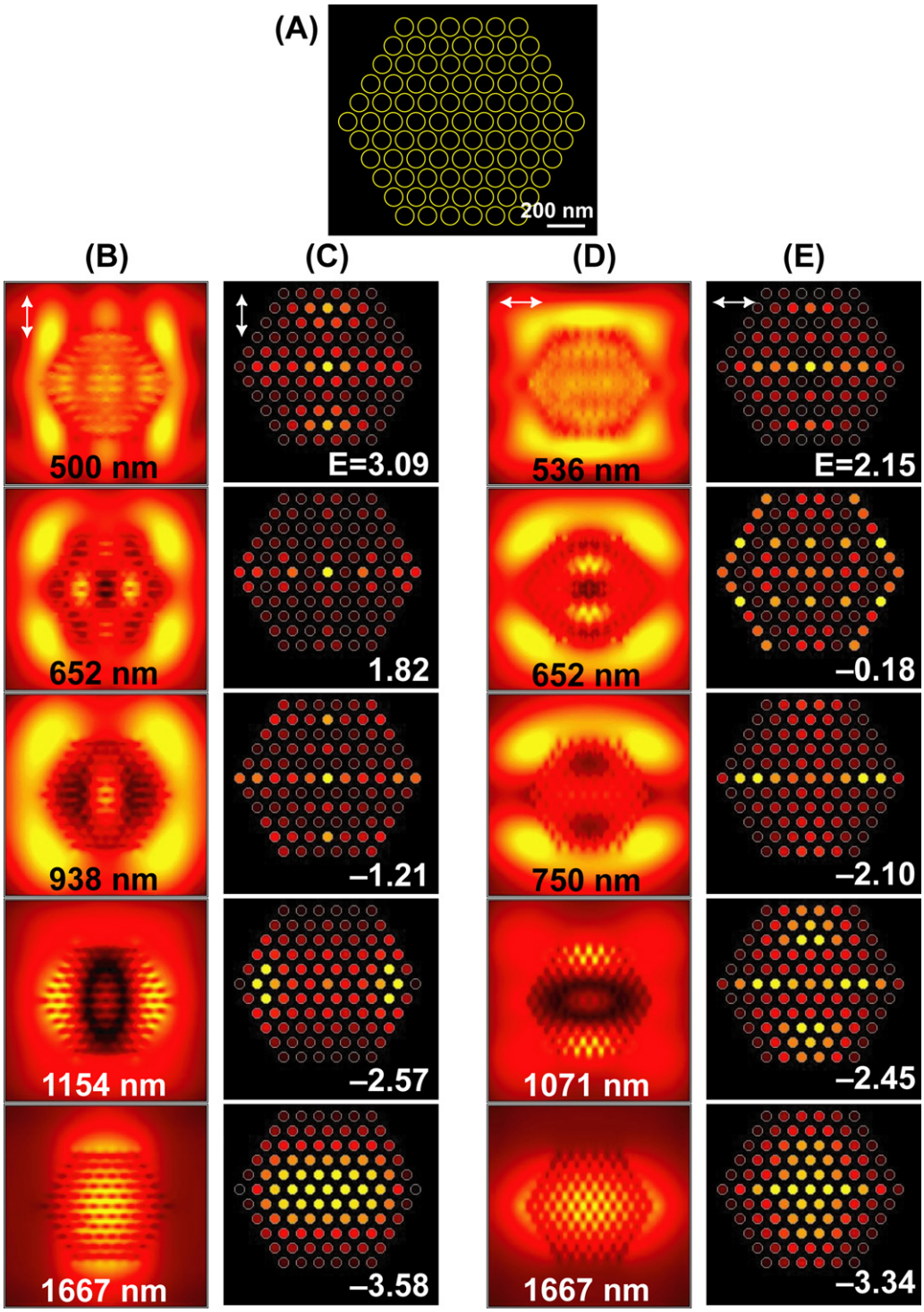

Fig. 1. (A) Model structure of monolayered assembly of gold nanospheres with a regular close-packed structure. The diameter of the nanosphere is 100 nm. (B) and (D) Representative field distributions calculated by finite-difference time-domain (FDTD) method, with incident polarizations in vertical (B) and horizontal (D) directions, as indicated by arrows. (C) and (E) Images of weighted local density-of-states calculated by the point dipole model (Eq. (3)), with vertical (C) and horizontal (E) polarizations (indicated by arrows).

are not induced in the inner parts. As a general characteristic of oscillation modes of a finite lattice with boundaries and/or defects, localized oscillation modes sometimes arise near the boundaries and/or defects [31,32]. It may be possible that the plasmon propagated from the inner part of the assembly is trapped at the rim due to the boundary-localized modes. In the island-like assemblies we observed, there may be localized modes in the rim part nearly resonant with the excitation wavelength, which may play some essential roles in the confined optical fields. It may be highly probable that the interparticle interaction as introduced in the point dipole model enables propagation of excitation in the assemblies, and as a consequence the enhanced fields are localized in the rim parts as found in the near-field images.

On the other hand, at lower frequencies, both FDTD simulation and the point dipole model give higher field amplitude or density of states, at the inner part of the assembly. This result is again consis-

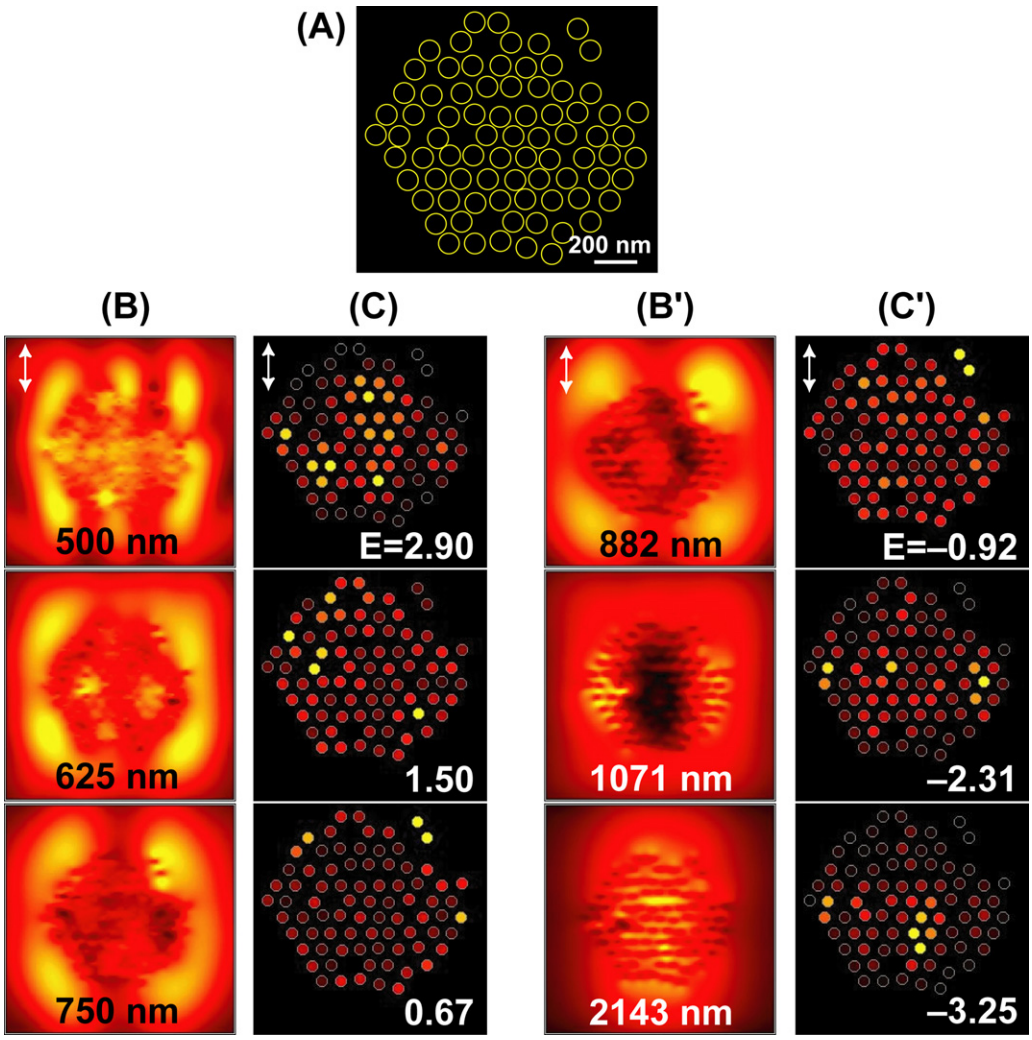

Fig. 2. (A) Model structure of monolayered assembly of gold nanospheres with a disordered structure. The diameter of the nanosphere is 100 nm. (B/B′) Representative field distributions calculated by FDTD method. The incident polarization is vertical (as indicated by arrows). (C/C′) Images of weighted local density-of-states calculated by the point dipole model. The polarization direction is vertical (indicated by arrows).

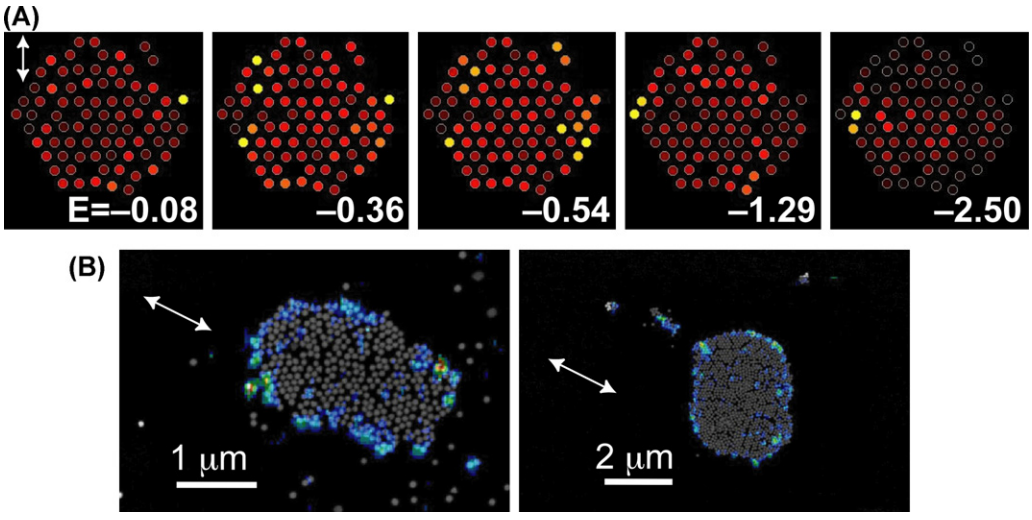

Fig. 3. (A) Representative images of local density of states calculated for the disordered assembly (Fig. 2A) by the point dipole model (Eq. (3)) in the frequency region between 0 and −2.5. The polarization direction is vertical (indicated by arrows). (B) Near-field two-photon excitation images of island-like assemblies of gold nanospheres (diameter 100 nm), overlaid by the scanning electron micrograph of the sample. The near-field two-photon excitation intensity is shown in a color scale, and the electron micrograph in black and white. The incident/detected polarization directions for the near-field measurements are indicated by arrows.

tent with a general feature of oscillation modes of a finite lattice. We may thus expect that such a spatial feature of the enhanced optical fields will be observed when the near-field two-photon excitation measurements in the longer wavelength region become achievable in the future.

4. Concluding remarks

In the present study, we qualitatively discussed the physical meaning of the characteristic feature found for the near-field two-photon excitation images of gold nanoparticle assemblies, i.e., confinement of enhanced optical fields at the rim parts of the island-like assemblies. For this purpose we conducted model calculations based upon FDTD method and the point dipole model, and compared the results with the near-field experimental results. The point dipole model incorporating the interparticle dipole–dipole interaction qualitatively reproduces the characteristic tendency of the FDTD calculation results, and the experimentally observed enhanced-field distribution as well. It is also of fundamental importance as the next step to investigate whether the simulation based on the point dipole model is consistent with the recently reported results on well-defined assemblies composed of several particles [17,18].

From the discussion given above, we may propose that the following points are important, to design efficient enhanced optical fields with metal nanoparticle assemblies. That is, close-packed arrangement of the particles does not usually yield highly enhanced field in a wide area of the assembly, and the enhanced fields are often localized at the rim parts and/or defects. For assemblies of many particles, in particular, the plasmon modes resonant with near-infrared radiation around 800 nm in most cases confine the enhanced fields in small areas. To get efficiently enhanced optical field in visible to near-infrared region, it is presumably advantageous to prepare assemblies with large fluctuation of the structure, containing many small-number assembly units (representatively dimers).

Acknowledgments

This work was partly supported by Grants-in-Aid for Scientific Research (Grant Nos. 18205004, 18685003, 22655007, and 22225002) from the Japan Society for the Promotion of Science and that on Priority Area “Strong Photon-Molecule Coupling Fields (Area No. 470, Grant No. 19049015) from the Ministry of Education, Culture, Sports, Science, and Technology of Japan.

References

[1] H. Xu, J. Aizpurua, M. Käll, P. Apell, Electromagnetic contributions to single-molecule sensitivity in surface-enhanced Raman scattering, Phys. Rev. E 62 (2000) 4318–4324.
[2] M. Futamata, Y. Maruyama, M. Ishikawa, Local electric field and scattering cross section of Ag nanoparticles under surface plasmon resonance by finite difference time domain method, J. Phys. Chem. B 107 (2003) 7607–7617.
[3] J. Jiang, K. Bosnick, M. Maillard, L. Brus, Single molecule Raman spectroscopy at the junctions of large Ag nanocrystals, J. Phys. Chem. B 107 (2003) 9964–9972.
[4] K. Li, M.I. Stockman, D.J. Bergman, Self-similar chain of metal nanospheres as an efficient nanolens, Phys. Rev. Lett. 91 (2003) 227402.
[5] E. Hao, G.C. Schatz, Electromagnetic fields around silver nanoparticles and dimers, J. Chem. Phys. 120 (2004) 357–366.
[6] C.E. Talley, J.B. Jackson, C. Oubre, N.K. Grady, C.W. Hollars, S.M. Lane, T.R. Huser, P. Nordlander, N.J. Halas, Surface-enhanced Raman scattering from individual Au nanoparticles and nanoparticle dimer substrates, Nano Lett. 5 (2005) 1569–1574.
[7] M. Moskovits, Surface-enhanced Raman spectroscopy: a brief retrospective, J. Raman Spectrosc. 36 (2005) 485–496.
[8] K. Yoshida, T. Itoh, H. Tamaru, V. Biju, M. Ishikawa, Y. Ozaki, Quantitative evaluation of electromagnetic enhancement in surface-enhanced resonance Raman scattering from plasmonic properties and morphologies of individual Ag nanostructures, Phys. Rev. B 81 (2010) 115406.
[9] L. Novotony, B. Hecht, Principle of Nano-Optics, Cambridge University Press, Cambridge, 2006.
[10] S.A. Maier, Plasmonics: Fundamentals and Applications, Springer, New York, 2007.
[11] K. Imura, H. Okamoto, M.K. Hossain, M. Kitajima, Near-field imaging of surface-enhanced Raman active sites in aggregated gold nanoparticles, Chem. Lett. 35 (2006) 78–79.
[12] K. Imura, H. Okamoto, M.K. Hossain, M. Kitajima, Visualization of localized intense optical fields in single gold–nanoparticle assemblies and ultrasensitive Raman active sites, Nano Lett. 6 (2006) 2173–2176.
[13] M.K. Hossain, T. Shimada, M. Kitajima, K. Imura, H. Okamoto, Raman and near-field spectroscopic study on localized surface plasmon excitation from the 2D nanostructure of gold nanoparticles, J. Microsc. 229 (Pt 2) (2008) 327–330.
[14] T. Shimada, K. Imura, M.K. Hossain, H. Okamoto, M. Kitajima, Near-field study on correlation of localized electric field and nanostructures in monolayer assembly of gold nanoparticles, J. Phys. Chem. C 112 (2008) 4033–4035.
[15] M.K. Hossain, T. Shimada, M. Kitajima, K. Imura, H. Okamoto, Near-field Raman imaging and electromagnetic field confinement in the self-assembled monolayer array of gold nanoparticles, Langmuir 24 (2008) 9241–9244.
[16] H. Okamoto, K. Imura, Near-field optical imaging of enhanced electric fields and plasmon waves in metal nanostructures, Prog. Surf. Sci. 84 (2009) 199–229.
[17] M. Hentschel, M. Saliba, R. Vogelgesang, H. Giessen, A.P. Alivisatos, N. Liu, Transition from isolated to collective modes in plasmonic oligomers, Nano Lett. 10 (2010) 2721–2726.
[18] J.A. Fan, C. Wu, K. Bao, J. Bao, R. Bardhan, N.J. Halas, V.N. Manoharan, P. Nordlander, G. Shvets, F. Capasso, Self-assembled plasmonic nanoparticle clusters, Science 328 (2010) 1135–1138.
[19] S.A. Maier, M.L. Brongersma, P.G. Kik, H.A. Atwater, Observation of near-field coupling in metal nanoparticle chains using far-field polarization spectroscopy, Phys. Rev. B 65 (2002) 193408.
[20] M.L. Brongersma, J.W. Hartman, H.A. Atwater, Electromagnetic energy transfer and switching in nanoparticle chain arrays below the diffraction limit, Phys. Rev. B 62 (2000) R16356–R16359.
[21] M. Suzuki, Y. Niidome, N. Terasaki, K. Inoue, Y. Kuwahara, S. Yamada, Surface-enhanced nonresonance Raman scattering of rhodamine 6G molecules adsorbed on gold nanorod films, Jpn. J. Appl. Phys. 43 (2004) L554–L556.
[22] H. Wang, C.S. Levin, N.J. Halas, Nanosphere arrays with controlled sub-10-nm gaps as surface-enhanced Raman spectroscopy substrates, J. Am. Chem. Soc. 127 (2005) 14992–14993.
[23] Y. Sawai, B. Takimoto, H. Nabika, K. Ajito, K. Murakoshi, Observation of a small number of molecules at a metal nanogap arrayed on a solid surface using surface-enhanced Raman scattering, J. Am. Chem. Soc. 129 (2007) 1658–1662.
[24] K. Ikeda, M. Takase, Y. Sawai, H. Nabika, K. Murakoshi, K. Uosaki, Hyper-Raman scattering enhanced by anisotropic dimer plasmons on artificial nanostructures, J. Chem. Phys. 127 (2007) 103–111.
[25] T. Kondo, F. Matsumoto, K. Nishio, H. Masuda, Surface-enhanced Raman scattering on ordered gold nanodot arrays prepared from anodic porous alumina mask, Chem. Lett. 37 (2008) 466–467.
[26] M.K. Hossain, Y. Kitahama, V. Biju, T. Itoh, T. Kaneko, Y. Ozaki, Surface plasmon excitation and surface-enhanced Raman scattering using two-dimensionally close-packed gold nanoparticles, J. Phys. Chem. C 113 (2009) 11689–11694.
[27] K. Ueno, S. Juodkazis, T. Shibuya, Y. Yokota, V. Mizeikis, K. Sasaki, H. Misawa, Nanoparticle plasmon-assisted two-photon polymerization induced by incoherent excitation source, J. Am. Chem. Soc. 130 (2008) 6928–6929.
[28] Y. Tsuboi, R. Shimizu, T. Shoji, N. Kitamura, Near-infrared continuous-wave light driving a two-photon photochromic reaction with the assistance of localized surface plasmon, J. Am. Chem. Soc. 131 (2009) 12623–12627.
[29] J.-P. Berenger, A perfectly matched layer for absorption of electromagnetic waves, J. Comput. Phys. 114 (1994) 185–200.
[30] P.B. Johnson, R.W. Christy, Optical constants of the noble metals, Phys. Rev. B 6 (1972) 4370–4379.
[31] J.D. Joannopoulos, R.D. Meade, J.N. Winn, Photonic Crystals: Molding the Flow of Light, Princeton University Press, Princeton, 1995.
[32] A.M. Kosevich, The Crystal Lattice: Phonons, Solitons, Dislocations Superlattices, 2nd ed., Wiley–VCH, Weinheim, 2005.